Microbiology (2009), **155**, 1523–1535 **DOI** 10.1099/mic.0.026500-0

The high-affinity phosphate transporter Pst in *Proteus mirabilis* HI4320 and its importance in biofilm formation

G. A. O'May,[1†] S. M. Jacobsen,[1†] M. Longwell,[2] P. Stoodley,[2] H. L. T. Mobley[3‡] and M. E. Shirtliff[1‡]

Correspondence
M. E. Shirtliff
mshirtliff@umaryland.edu

[1]Department of Microbial Pathogenesis, University of Maryland – Baltimore, Dental School, 650 W. Baltimore Street, Baltimore, MD 21201, USA

[2]Center for Genomic Sciences, Allegheny-Singer Research Institute, 320 East North Avenue, Pittsburgh, PA 15212, USA

[3]Department of Microbiology and Immunology, University of Michigan Medical School, Ann Arbor, MI 48109, USA

Proteus mirabilis causes urinary tract infections (UTIs) in individuals requiring long-term indwelling catheterization. The pathogenesis of this uropathogen is mediated by a number of virulence factors and the formation of crystalline biofilms. In addition, micro-organisms have evolved complex systems for the acquisition of nutrients, including the phosphate-specific transport system, which has been shown to be important in biofilm formation and pathogenesis. A functional Pst system is important during UTIs caused by *P. mirabilis* HI4320, since transposon mutants in the PstS periplasmic binding protein and the PstA permease protein were attenuated in the CBA mouse model of UTI. These mutants displayed a defect in biofilm formation when grown in human urine. This study focuses on a comparison of the proteomes during biofilm and planktonic growth in phosphate-rich medium and human urine, and microscopic investigations of biofilms formed by the *pst* mutants. Our data suggest that (i) the Δ*pst* mutants, and particularly the Δ*pstS* mutant, are defective in biofilm formation, and (ii) the proteomes of these mutants differ significantly from that of the wild-type. Therefore, since the Pst system of *P. mirabilis* HI4320 negatively regulates biofilm formation, this system is important for the pathogenesis of these organisms during complicated UTIs.

Received 5 December 2008
Revised 21 January 2009
Accepted 23 January 2009

INTRODUCTION

Proteus mirabilis – a member of the family *Enterobacteriaceae* – is the most common aetiological agent responsible for complicated urinary tract infections (UTIs) (Mobley, 1996). Subpopulations at higher risk for infection by this pathogen include those with long-term indwelling catheterization as well as those with structural and functional abnormalities within the urinary tract (Mobley, 1996). Clinical syndromes associated with *P. mirabilis* include cystitis and pyelonephritis, with possible complications from stone formation and bacteraemia (Mobley, 1996). These micro-organisms survive in the urinary tract by virtue of their production of a battery of virulence factors, including urease, flagella, fimbriae, haemolysin and IgA protease (Belas, 1996; Mobley *et al.*, 1994; Musher *et al.*, 1975; Peerbooms *et al.*, 1984; Walker *et al.*, 1999), and formation of crystalline biofilm on indwelling catheters (Stickler *et al.*, 1993).

Biofilm formation – one of the most important mechanisms of pathogenicity of this micro-organism in the urinary tract – may be defined as a community of surface-attached bacteria encased in an extracellular matrix consisting of secreted carbohydrates, proteins and DNA. Indeed, biofilms have been associated with the virulence of a number of pathogens (Castelli *et al.*, 2006). Organisms in these communities display phenotypic differences from planktonic cells, including a slower rate of growth and increased resistance to antibiotics (Lewis, 2001; Stoodley *et al.*, 2002). *P. mirabilis* biofilms in urine are unique in that the extracellular polysaccharide matrix is enmeshed with struvite and carbonate apatite crystals (Jones *et al.*, 2006).

†These authors contributed equally towards completion of this study.

‡These authors contributed equally towards completion of this study.

Abbreviations: CLSM, confocal laser scanning microscopy; 2DGE, 2D gel electrophoresis; UTI, urinary tract infection.

Two supplementary figures, showing 2D gel electrophoresis images of the proteome of *P. mirabilis* HI4320 cultured planktonically in LB, with and without annotation, are available with the online version of this paper.

Crystal formation occurs due to the urease-catalysed hydrolysis of urea into ammonia, leading to an increase in the local pH and the precipitation of calcium, magnesium and phosphate ions (Morris *et al.*, 1999). The pathogenesis of *P. mirabilis* UTIs is not at present understood fully.

The Pst system of *P. mirabilis* (Table 1), a multimeric, high-affinity inorganic phosphate (P_i) transporter, is induced at limiting extracellular P_i concentrations (<1 mM, K_m^{app} of 0.2 μM) (Rao & Torriani, 1990; Rosenberg *et al.*, 1977). *pst* mutants are highly attenuated in cochallenge colonization of the CBA mouse model (Burall *et al.*, 2004; Jacobsen *et al.*, 2008). *P. mirabilis* HI4320 possesses a *pst* operon identical in gene organization to that observed in *Escherichia coli*. Previous studies have suggested that the roles of the Pst transport system in pathogenesis include regulation of invasion (Lucas *et al.*, 2000; Mathew *et al.*, 2001; Sinai & Bavoil, 1993), antibiotic resistance (Soualhine *et al.*, 2005), colonization (Buckles *et al.*, 2006; Daigle *et al.*, 1995; Lamarche *et al.*, 2005; Orihuela *et al.*, 2001; Peirs *et al.*, 2005; Runyen-Janecky *et al.*, 2005), and biofilm formation (Monds *et al.*, 2001).

Since (i) earlier work has alluded to the importance of this system during biofilm formation (Monds *et al.*, 2001, 2007) and (ii) the formation of crystalline biofilms is a characteristic of UTIs associated with *P. mirabilis*, we hypothesized that the Pst system of *P. mirabilis* HI4320 is involved in biofilm formation during establishment of a UTI. To assess the role of the Pst system, this study focused upon determining previously undetected *in vitro* phenotypes of the Δ*pst* mutants by comparing biofilm formation between the wild-type HI4320 and Δ*pstA and* Δ*pstS* mutants via confocal laser scanning microscopy (CLSM) and quantitative analysis of surface coverage, and by comparing *in vitro* protein expression of these strains grown planktonically and as a biofilm.

METHODS

Bacterial strains, plasmids, reagents and culture conditions. Bacterial strains and plasmids used in this study are listed in Table 2. Wild-type *P. mirabilis* HI4320 was isolated from the urine of a long-term-catheterized elderly woman with significant bacteriuria ($\geqslant 10^5$ c.f.u. ml^{-1}) (Mobley & Warren, 1987; Warren *et al.*, 1982). Δ*pst* mutants used in this study, G1-43 (Δ*pstA*) and H4-34 (Δ*pstS*), were generated previously by signature-tagged mutagenesis and were polar mutants (Burall *et al.*, 2004) (Fig. 1). All plasmids were initially constructed in either *E. coli* DH5α (Bethesda Research Laboratories) or *E. coli* TOP10 (Invitrogen).

All reagents were manufactured by Fisher Scientific, Sigma-Aldrich, American Bioanalytical, Amersham Biosciences or J. T. Baker. Multimark protein molecular mass marker was purchased from Invitrogen. PBS, urea, thiourea, Biuret solution, Folin reagent, bromophenol blue, TCA, sodium thiosulfate, iodoacetamide, formaldehyde and PMSF were obtained from Sigma Aldrich. Immobiline Dry Strips (18 cm, pH 3–10, nonlinear), Pharmalytes (pH 3–10), mineral oil, DTT, CHAPS, the Multiphor II isoelectric focuser and the Höefer DALT Vertical System were obtained from Amersham Biosciences. Most other chemicals and media, including acrylamide (40 %), silver nitrate, sodium carbonate, SDS, ammonium persulfate, yeast extract, NaCl, Tris base and agarose, were obtained from Fisher Scientific. Tetramethylethylenediamine (TEMED) was obtained from

Table 1. Characteristics of the *P. mirabilis pst* operon

Gene	pI	MW (kDa)	Function	Cellular location
pstS	8.71	37.0	Phosphate binding; domain from amino acid residues 27 to 319	Periplasmic space
pstC	5.27	34.6	Cytoplasmic membrane permease with six predicted transmembrane domains	Cytoplasmic membrane
pstA	9.95	33.1	Cytoplasmic membrane permease with six predicted transmembrane domains	Cytoplasmic membrane
pstB	6.34	29.1	ATPase; domain from amino acid residues 36 to 230	Multiple
phoU	5.28	27.9	*pho* regulon negative regulator protein	Cytoplasm

Table 2. Bacterial strains and plasmids used in this study

Strain or plasmid	Description	Source
***P. mirabilis* strains**		
HI4320	Wild-type *P. mirabilis* isolate, Tet^r	Mobley & Warren (1987)
G1-43 (Δ*pstA*)	*pstA* mutant of HI4320 (*pstA*::Tn*5* Kan^r)	Burall *et al.* (2004)
H4-34 (Δ*pstS*)	*pstS* mutant of HI4320 (*pstS*::Tn*5* Kan^r)	Burall *et al.* (2004)
Plasmids		
pKHKS403	Moderate-copy-number cloning vector used for complementation, 3159 kb, pBluescript with p15A ori from pACYC184, Amp^r	H. L. T. Mobley
pSMJ003	pKHKS403 with *pstS-phoU* (*pst* operon)	Jacobsen *et al.* (2008)

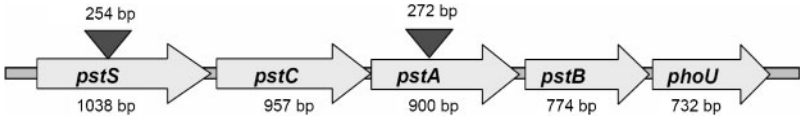

Fig. 1. The *pst* operon of *P. mirabilis*, showing the position and size of the Δ*pstA* and Δ*pstS* insertion sites.

Bio-Rad. Zirconia/silica 0.1 mm beads were purchased from Biospec Products. Components of the bacterial culture medium were purchased from Becton Dickinson.

Luria broth (LB; containing, per litre, 10 g tryptone, 5 g yeast extract and 10 g NaCl) was used routinely with the appropriate antibiotics (15 μg tetracycline ml^{-1}, 50 μg kanamycin ml^{-1} and/or 100 μg ampicillin ml^{-1}) to culture *P. mirabilis*. Urine was collected from multiple anonymous healthy donors, pooled, filter-sterilized and stored in the dark at 4 °C until required.

Growth of planktonic *P. mirabilis in vitro*. An overnight culture of either *P. mirabilis* HI4320 or Δ*pst* mutants in LB and appropriate antibiotics was diluted 1 : 40 into fresh LB without antibiotics and incubated at 37 °C with shaking at 200 r.p.m. for 2 h. This was diluted 1 : 200 into 100 ml test medium and incubated at 37 °C with shaking. For the studies examining growth in LB, each strain was incubated at 37 °C until OD_{600} 0.3–0.4 was reached. For comparisons of growth in LB against that in pooled human urine, cultures were incubated at 37 °C for 24 and 48 h to ensure growth but limit crystal formation. After the required period, cultures were pelleted and resuspended in protein preservation solution (2.8 mM PMSF, 10 mM Tris/HCl and 1 mM EDTA, pH 8.0) to prevent protein degradation and changes in protein expression.

Growth of *P. mirabilis* biofilm *in vitro*. A variation of the *in vitro* flow reactor system utilized in our laboratory for *Staphylococcus aureus* biofilm culture (Brady *et al.*, 2006) was used. The reactor system was constructed within a 37 °C incubator and consisted of silicone tubing through which pooled human urine (pH 5.0–6.5) flowed under the control of a peristaltic pump into a waste container. This system incorporated square-cross-section glass flow cells for use in confocal microscopy studies. Prior to inoculation, urine was pumped through the system and allowed to equilibrate to temperature for 24 h. An overnight culture of *P. mirabilis* HI4320 or Δ*pst* mutants grown in LB and appropriate antibiotics was diluted 1 : 100 into fresh LB without antibiotics and allowed to grow at 37 °C with shaking for 2 h. The tubing was clamped upstream of the injection ports and 1.0 ml exponential phase bacterial culture was injected. The system was incubated without flow for 20 min at 37 °C so that bacteria could adhere to the luminal surface. The media flow was restored to a flow rate of 0.5 ml min^{-1} at 37 °C for 21 h. At 21 h, biofilm was harvested by (i) removal of the square glass flow cells for confocal microscopy and (ii) squeezing the biofilm from the tubing into protein preservation solution for protein expression analysis. Total biofilm protein was collected by mechanical disruption using a FastPrep instrument (Qbiogene) with 0.1 mm zirconia/silica beads and quantified using the modified method of Bradford (Bradford, 1976).

2D gel electrophoresis (2DGE). 2DGE was conducted according to the principles of O'Farrell (1975) and as outlined by Gorg *et al.* (2000) and Sauer & Camper (2001). Rehydration of 400 μg crude protein was accomplished by the addition of a one-tenth volume of ice-cold 1 : 10 TCA : acetone. The resulting pellet was solubilized in rehydration buffer (0.1 mM urea, 25 μM thiourea, 0.35 μM DTT, 0.5 %, w/v, CHAPS, 1.6 % Pharmalyte, pH 3–10). These samples were applied to 18 cm, pH 3–10 (nonlinear), Immobiline Dry-Strips (GE Healthcare) and allowed to swell at room temperature for at least 23 h prior to focusing. IEF was performed using a Multiphor II from Amersham as per the manufacturer's directions. Prior to the second dimension, the immobilized pH gradient (IPG) strips were equilibrated (as per the manufacturer's directions) and subsequently applied to the top edge of the 26 cm × 20 cm 2D Höefer DALT Vertical System gel system (Amersham Biosciences). Crude protein extracts were separated at 10 °C on an 11 % resolving gel, which was then non-destructively silver-stained (Gharahdaghi *et al.*, 1999).

MALDI-TOF analysis. Protein spots excised from 2D-PAGE gels were sent for processing and analysis at the Mass Spectrometry Core of the Biomolecular Resource Facility at the University of Texas Medical Branch. For identification of trypsin-digested proteins, an Applied Biosystems Voyager-DE STR MALDI-TOF mass spectrometer or Applied Biosystems 4800 MALDI-TOF/TOF mass spectrometer was operated in the positive-ion mode with α-cyano-4-hydroxycinnamic acid matrix used for ionization. At least 100 laser shots per spectrum were averaged. Mass spectral peaks with a signal-to-noise ratio greater than 5 : 1 were deisotoped, and the resulting mono-isotopic masses were used for protein identification using mass fingerprint analysis. Proteins were identified by correlation of uninterpreted tandem mass spectra to entries in the database PAHI4320 completefirstrun.2005.01.16, utilizing the ProteinProspector MS-Fit server (IBM AIX version, University of California at San Francisco; http://prospector.ucsf.edu/) (Clauser *et al.*, 1999). This database was generated by GLIMMER [Gene Locator and Interpolated Markov modelER; The Institute For Genomic Research (TIGR); http://www.tigr.org/software/glimmer/] (Delcher *et al.*, 1999) from the nucleotide sequence available from the Sanger Centre, Cambridge, UK (http://www.sanger.ac.uk/Projects/P_mirabilis/). For the initial pass search, no mass or pI constraints were applied and one missed cleavage per peptide was allowed. The mass tolerance for the monoisotopic precursor ion was set at ±50 p.p.m. All matching spectra were reviewed manually, and proteins with an expectation MOWSE score of 10 or more were considered positive identities. Protein spot comparisons and analysis were accomplished using the Image-MASTER 2D Platinum software (Amersham Biosciences, version 5.00) and Melanie 3 software (GeneBio). Determination of proteins that were exclusively expressed in either the HI4320 strain or the *pst* mutants was accomplished through analysis of the Melanie-generated spot report and confirmation through the appearance of the protein spot in at least three separate gels. Functional and cellular localization predictions were accomplished using the KEGG GENES database (Kyoto Encyclopedia of Genes and Genomes; http://www.genome.ad.jp/kegg/genes.html) and PSORT-B v.2.0 (http://www.psort.org/; Gardy *et al.*, 2003), respectively.

Biofilm formation assay. To assess biofilm formation during static conditions, an adaptation of the 96-well microtitre dish biofilm assay developed by O'Toole and co-workers (O'Toole & Kolter, 1998; O'Toole *et al.*, 1999) based on viable counts was performed. An overnight culture of *P. mirabilis* HI4320 and the Δ*pst* mutants was diluted 1 : 40 into fresh LB and allowed to grow at 37 °C with shaking for 2 h. Pooled human urine was inoculated with 25 μl of each 2 h culture into polystyrene six-well plates (Becton Dickinson) in triplicate. Samples were incubated at 37 °C statically and after 24 h, growth medium was replaced with fresh urine. After 48 h, excess urine was discarded from each well and 1.0 ml PBS was added to remove any planktonic culture that remained. Well bottoms were scraped to remove biofilms; these were resuspended in PBS. Biofilm suspension was diluted 1 : 10 in PBS and homogenized with the Polytron Pt 1200 CL homogenizer (Kinematica), probe set 5 for 30 s. Bacterial counts (c.f.u. ml^{-1}) for the 48 h samples were determined

by diluting samples 10-fold in PBS and plating each dilution on Luria agar plates.

CLSM. To determine whether mutations in the Pst system of *P. mirabilis* HI4320 affect biofilm formation under flow conditions, visualization of the wild-type and mutant strains was accomplished through differential viability staining and CLSM. Biofilms were grown under flow in pooled human urine as described above. Prior to staining, flow cells were washed with 0.85 % NaCl to remove excess urine. Bacterial cells were stained in the dark for at least 15 min at room temperature with 3 ml BacLight Live/Dead stain (3.34 mM SYTO 9, 20 mM propidium iodide in 0.85 %, w/v, NaCl; Molecular Probes, Invitrogen). Samples were washed in fresh 0.85 % (w/v) NaCl and then visualized using an LSM510 Meta laser scanning confocal microscope (Carl Zeiss). The microscope was configured with two lasers (argon 488 nm/514 nm/543 nm and HeNe 633 nm) and micrographs were taken at random with the Plan-Apochromat ×20/0.75 lens or, if otherwise noted, with the Plan Neofluar ×10/0.3 lens. Green fluorescence was used as an indicator of the presence of living cells in the biofilm, as SYTO 9 (480 nm excitation) is a freely diffusible nucleic acid intercalator that labels all cells in the microbial population regardless of viability. To distinguish viable cells from dead organisms, the membrane-impermeant DNA intercalator propidium iodide (536 nm excitation) was used as a counterstain to stain cells with compromised membrane integrity. A series of horizontal (*xy*) optical sections were taken throughout the full-length of the biofilm. Image capture and 2D projections of *z*-stacks were performed using the LSM 510 Meta image acquisition software (Zeiss). The subsequent micrographs were analysed quantitatively for biomass, mean and maximum thickness, and roughness coefficient using the Community Statistics (COMSTAT) image analysis software (Heydorn *et al.*, 2000).

Statistical analyses. The Student's *t* test was used to determine significant differences in biofilm growth throughout all of the biofilm plate assays; a P value <0.05 was considered statistically significant. All determinations were performed in triplicate.

RESULTS

Biofilm formation by *P. mirabilis* HI4320 and its *pst* mutants

Since it has been shown that biofilm formation plays a role in early *P. mirabilis* UTIs and that gene products of the *pst* operon negatively regulate biofilm formation (Monds *et al.*, 2001), quantitative biofilm microtitre assays were performed. After 48 h of static growth in pooled human urine, a 2.5- and eightfold reduction in biofilm formation between the HI4320 wild-type and the Δ*pstA* and Δ*pstS* mutants, respectively, was observed [wild-type, 1.65×10^7 c.f.u. ml^{-1}; Δ*pstA*, 6.6×10^6 c.f.u. ml^{-1} (P=0.03); Δ*pstS*, 2.1×10^6 c.f.u. ml^{-1} (P=0.02); Fig. 2]. These data suggest that biofilm formation is impaired in the Δ*pstA* and Δ*pstS* mutants.

Comparison of biofilm formation by CLSM

Visualization of 21 h flow-grown biofilms by CLSM and BacLight staining revealed differences in surface coverage and biofilm architecture between the wild-type strain and the Δ*pst* mutants (Fig. 3). Wild-type HI4320 biofilms, grown in human pooled urine, possess a dense 3D organization consisting of towering mushroom structures with water channels flowing throughout. Conversely, the biofilms formed by the Δ*pst* mutants lacked this distinct 3D architecture and were composed only of large, irregularly shaped microcolonies/aggregates (Fig. 3). These images revealed that the Δ*pst* mutants are defective in biofilm formation as compared with the wild-type strain and apparently cannot form mature biofilm structures under flow conditions during growth in pooled human urine.

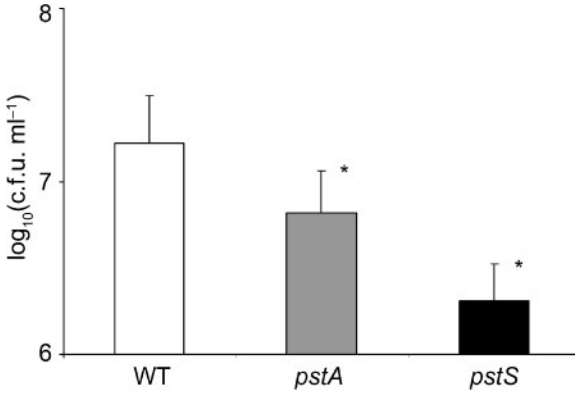

Fig. 2. Viable cell count biofilm assay comparing 48 h biofilm formation during growth in pooled human urine between wild-type *P. mirabilis* HI4320 and the Δ*pstA* and Δ*pstS* mutants. Bacterial counts [in $\log_{10}$(c.f.u. cm^{-1})] were determined by serial dilution and spread plating. Data are presented as mean ± SD of triplicate assays; asterisks denote statistically significant differences ($P<0.05$).

To quantify the data obtained from the CLSM images, COMSTAT analysis software was used to assess the quantity (biomass, and mean and maximum thickness) and quality of the biofilms (roughness coefficient) grown under flow in pooled human urine. CLSM images of a single biofilm (total images; HI4320, 97; Δ*pstA*, 49; Δ*pstS*, 42) were taken randomly and converted into black and white for analysis by this software. Quantitative computer analysis of biofilm architecture using COMSTAT verified visual observations, as biofilms formed by Δ*pst* mutants grown in pooled human urine differed from wild-type biofilm with respect to mean and maximum thickness (μm) as well as total biomass (Table 3). Under flow conditions, biofilms formed by the Δ*pstS* mutant during growth in pooled human urine demonstrated a reduction in biomass as compared with the HI4320 wild-type strain (Table 3; Δ*pstS*, 0.04 μm^3 μm^{-2}; Δ*pstA*, 1.40 μm^3 μm^{-2}; HI4320, 1.21 μm^3 μm^{-2}). These findings, in conjunction with the other biofilm analyses, indicate that mutants in the Pst system of *P. mirabilis* HI4320 are defective in biofilm formation. As stated previously, the Δ*pst* mutants are defective in biofilm formation as compared with the wild-type strain as visualized by CLSM, and apparently these mutants cannot form mature biofilm structures.

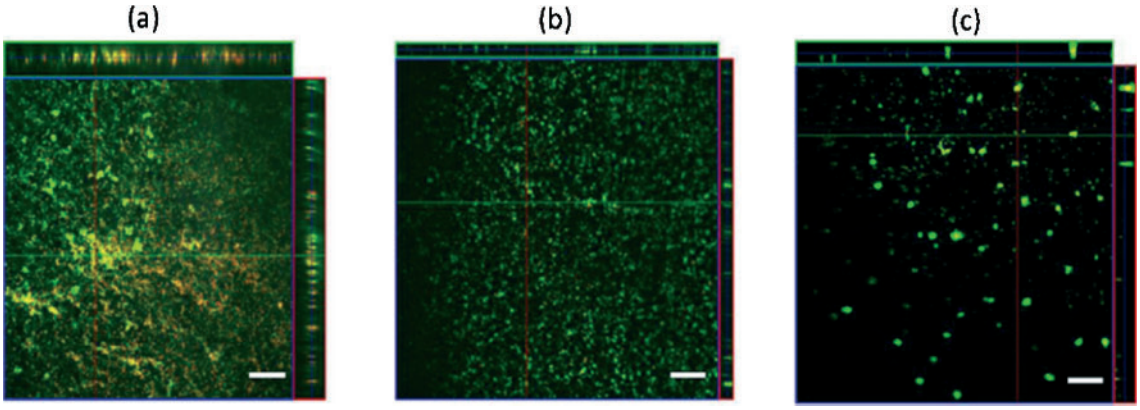

Fig. 3. CLSM images of wild-type *P. mirabilis* HI4320 and Δ*pst* mutant biofilms grown under flow in pooled human urine. Biofilms on glass flow cells were stained with Live/Dead stain and images were captured using a Plan-Apochromat ×20/0.75 lens, except for the side views (Plan-Neofluar ×10/0.3). (a) Wild-type *P. mirabilis*, stack size 460.7×460.7×48.0 μm; (b) Δ*pstA* mutant *P. mirabilis*, stack size 651.5×651.5×24.5 μm; (c) Δ*pstS* mutant *P. mirabilis*, stack size 651.5×651.5×42.0 μm. Lines in the *xy* plane depict the location of *z* projections, 97, 49 and 42 μm deep, respectively, shown at the top and right of the images. Bars, 50 μm.

Table 3. COMSTAT analysis of the wild-type HI4320 and *pst* mutant strains after 21 h biofilm growth in pooled human urine

Strain	Biomass ($\mu m^3\ \mu m^{-2}$)*	Mean thickness (μm)†	Maximum thickness (μm)‡	Roughness coefficient§
Wild-type	1.21	2.70	25.0	1.83
pstA	1.40	2.46	17.33	1.72
pstS	0.04‖	0.07‖	5.63‖	1.97

*A measurement of the overall volume of the biofilm.
†A measurement of the spatial area occupied by the biofilm.
‡A measurement of the maximum thickness at a given location in the biofilm.
§A measurement of variation in biofilm thickness and an indicator of biofilm heterogeneity.
‖Statistically significant difference ($P<0.05$).

Proteomic comparison of *P. mirabilis* HI4320 and the *pst* mutants

Proteomic analysis using 2DGE was used to compare the wild-type HI4320 strain with the Δ*pst* mutants grown as a biofilm in pooled human urine (Fig. 4, Table 4) and planktonically in LB in phosphate-excess conditions (Figs 5 and 6, Table 5).

Biofilm growth in pooled human urine

Comparisons of the proteomes of the HI4320 and the *pst* mutant biofilms cultured under flow in pooled human urine were performed (Fig. 4, Table 4). A total of 18 proteins were tentatively identified as being exclusively expressed (16 proteins in the Δ*pst* mutants, two proteins in the HI4320 strain) (Table 4). Four proteins (AnsB, AphA, PstS and PepE; Table 4) were expressed in the Δ*pstA* mutant but not in Δ*pstS*. Sixteen proteins were present only in the Δ*pst* mutant strains and not in the wild-type (Table 4). Three were known members of the *pho* regulon (alkaline phosphatase PhoA, PstS and glycerol 3-phosphate periplasmic binding protein UgpB) and would be expected to be upregulated in these Δ*pst* mutant strains. The other proteins were identified as performing a variety of functions (Table 4). Four were found to be involved in nutrient scavenging, including the proline aminopeptidase PepP, the α-aspartyl dipeptidase PepE, the aminobenzoyl-glutamate utilization protein AbgA, and the deoxyribose-phosphate aldolase DeoC. One protein, ArnB, is an amino transferase known to be involved in LPS biosynthesis. Two proteins, the class B acid phosphatase AphA and the acetoin reductase BudC, are known to be involved in the prevention of intracellular acidification. Two were identified only as putative proteins (2-hydroxyacid dehydrogenase YcdW and PMI1966), and three other proteins are known to be involved in general

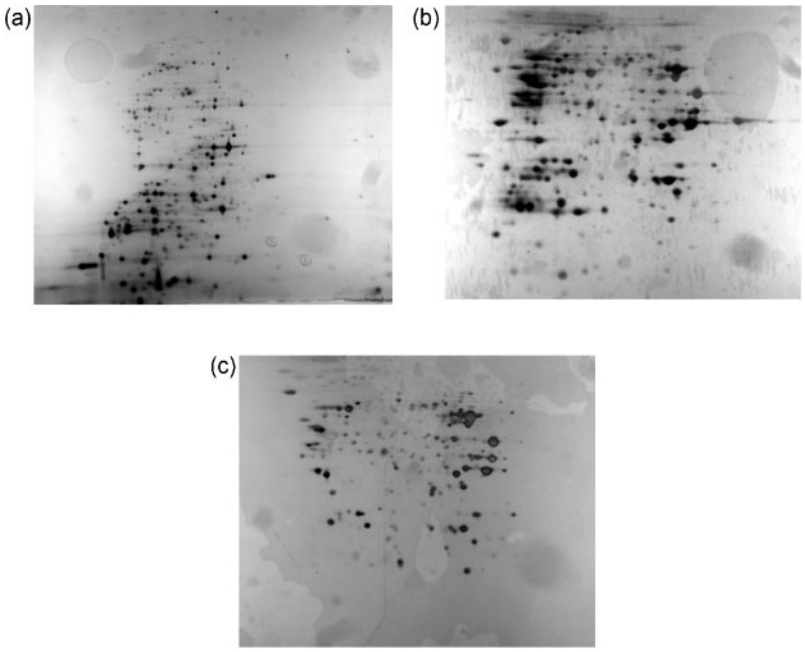

Fig. 4. Proteomic comparison of the wild-type HI4320 strain and the Δ*pst* mutant strains after biofilm growth in pooled human urine, as visualized by 2D PAGE. Overnight cultures were utilized to inoculate pooled human urine and grown in a biofilm flow reactor system for 21 h. After standardization, whole-cell lysates were prepared and 400 μg protein was loaded. pH range 3–10 was utilized, with pH 3 on the left. Protein spots were excised and examined by MALDI-TOF or MALDI-TOF/TOF. (a) HI4320, (b) Δ*pstA*, (c) Δ*pstS*.

metabolism (phosphoglycerate kinase Pgk, seryl-tRNA synthetase SerS and L-asparaginase II AnsB). Some proteins expressed in the mutants have been demonstrated in other studies to be indirectly associated with the downregulation of biofilm formation (NagB, AphA). These analyses provide some insight as to which systems are affected by mutations in the *pst* operon.

Two proteins, the 70 kDa heat-shock protein DnaK and the cytosol aminopeptidase PepA, were expressed exclusively in

Table 4. Proteins of the wild-type and *pst* mutant strains expressed exclusively during biofilm growth in pooled human urine

PMI number*	Protein	Function	Cellular location
Proteins upregulated in *pst* mutants only			
242	Pgk	Phosphoglycerate kinase	Cytoplasm
454	NagB	Glucosamine-6-phosphate isomerase	Unknown
700	SerS	Glycine, serine, threonine metabolism	Cytoplasm
708†	AnsB	L-Asparaginase II	Periplasm
729†	AphA	Class B acid phosphatase precursor	Unknown
1043	ArnB	PbgP1 protein	Cytoplasm
1094	YcdW	2-Hydroxyacid dehydrogenase	Cytoplasm
1966	–	NADPH-dependent FMN reductase protein	Unknown
2024	PepP	Proline aminopeptidase	Cytoplasm
2092	BudC	Acetoin phosphatase	Cytoplasm
2416	DeoC	Deoxyribose-phosphate aldolase	Cytoplasm
2500	PhoA	Alkaline phosphatase	Periplasm
2893	PstS	Phosphate-binding periplasmic protein precursor	Periplasm
3545†	PepE	α-Aspartyl dipeptidase	Cytoplasm
3617	UgpB	Glycerol 3-phosphate-binding periplasmic protein	Periplasm
3674	AbgA	Aminobenzoyl-glutamate utilization protein	Unknown
Proteins upregulated in the wild-type only			
9	DnaK	Heat-shock protein 70 chaperone protein DnaK	Cytoplasm
3464	PepA	Cytosol aminopeptidase A/I	Cytoplasm

*PMI – *Proteus mirabilis* index; a *P. mirabilis* genome databank hosted at the Sanger Institute, Cambridge, UK; http://www.sanger.ac.uk/Projects/P_mirabilis/.
†Expressed only in the *pstA* mutant. Proteins with no designation were left blank.

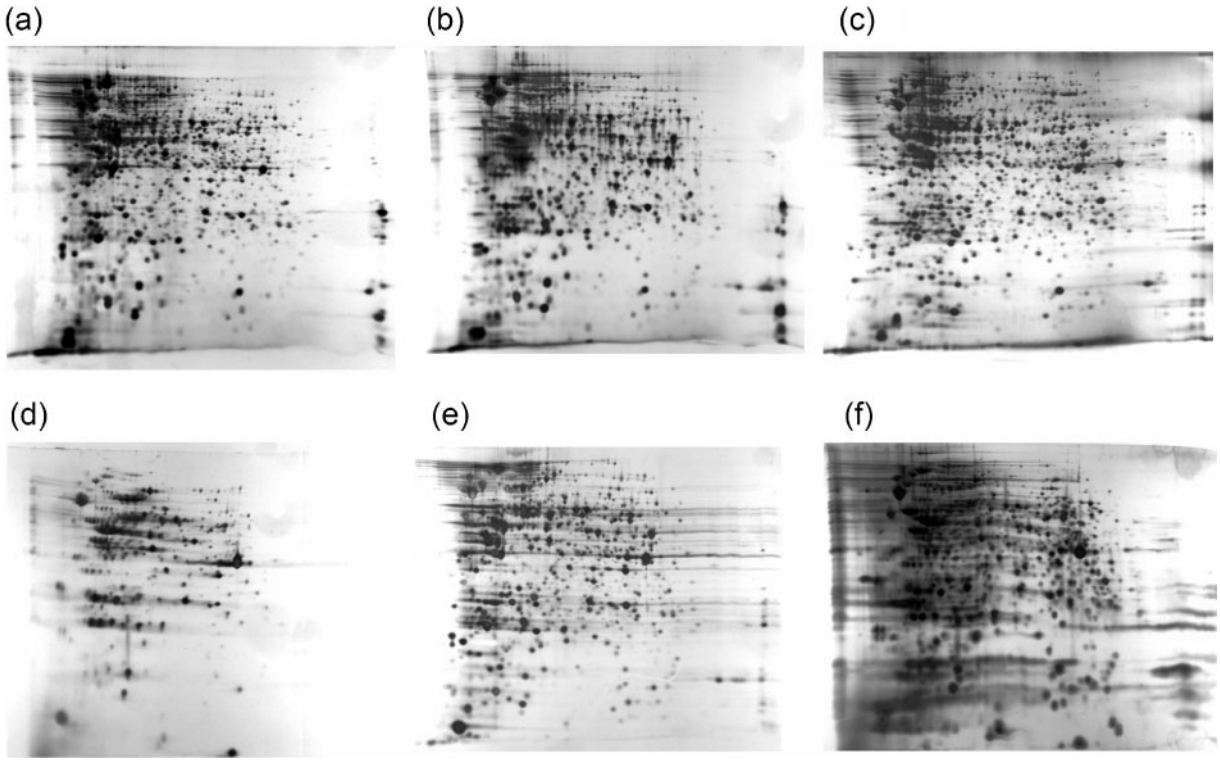

Fig. 5. Proteomic comparison of the wild-type HI4320 strain and the *pst* mutant strains during planktonic growth in LB, as visualized by 2D PAGE. pH range 3–10 was utilized, with pH 3 on the left. Six hundred and sixty-nine spots were excised and examined by MALDI-TOF or MALDI-TOF/TOF. Samples were run at least in triplicate. (a) HI4320, (b) Δ*pstS*, (c) Δ*pstA*, (d) HI4320(pKHKS403), (e) Δ*pstS*(pKHKS403), (f) Δ*pstA*(pKHKS403).

the HI4320 strain. Currently, there are no known roles for these proteins during biofilm formation. Thus, they may assist the organism in adapting to growth in human urine.

Planktonic growth in LB

Proteomes of the HI4320 strain, the Δ*pst* mutants, and the latter strains transformed with the pKHKS403 vector possessing the complete *pst* operon, were compared after planktonic growth in phosphate-rich LB (Figs 5 and 6, Supplementary Figs S1 and S2). A total of 32 proteins were exclusively expressed in either the wild-type (22 proteins) or mutant (10 proteins) strains (Table 5). Of the 22 proteins that were identified as being exclusively upregulated in the wild-type, several are associated with amino acid metabolism and translation, such as the amino acid transporter protein OppA1, the glycine cleavage enzyme GcvT, the enzyme IlvG, the peptidase PepQ, the 50S ribosomal subunit protein L6 RplF, the tRNA pseudouridine synthases TruB and TruD, and the putative glutathionylspermidine synthase YgiC. A number of transcriptional regulators were expressed by this strain, including a putative MerR-family regulator, an IclR transcriptional regulator, KdpE, and NtrB. Other metabolic proteins that were exclusively expressed included the long-chain fatty acid transporter FadL, the aspartate carbamoyltransferase PyrB, the cold-shock RNA helicase DeaD (nucleotide metabolism), the tellurite-resistance protein TerB, and the coenzyme lipoic acid synthesis protein LipA. Three putative proteins were expressed in the HI4320 strain (putative lipoprotein 2631, hypothetical protein 2798, DNase YcfH). Proteins involved in carbohydrate metabolism were identified and included the 3-carboxymuconate cyclase YbhE and the putative gluconokinase GntK.

A variety of proteins were upregulated exclusively in the *pst* mutants, including phosphate assimilation and transport proteins (UgpB, UgpC, UgpQ, PhnX and PstS), the ribosomal recycling factor Frr, the oligoRNase Orn and two hypothetical proteins (PMI3296 and PMI3715). As expected, the PstS protein was expressed only in the Δ*pstA* mutant (Fig. 6, Table 5). Introduction of the complete *pst* operon into the Δ*pst* mutants demonstrated that complementation occurred: known members of the *pho* regulon (UgpB, UgpC, PstS and PhnX) were downregulated in these strains (Fig. 6, Table 5).

These data suggest that mutations in the *pst* system of *P. mirabilis* HI4230 have an effect on global protein expression; several proteins were present or absent in these mutants, as

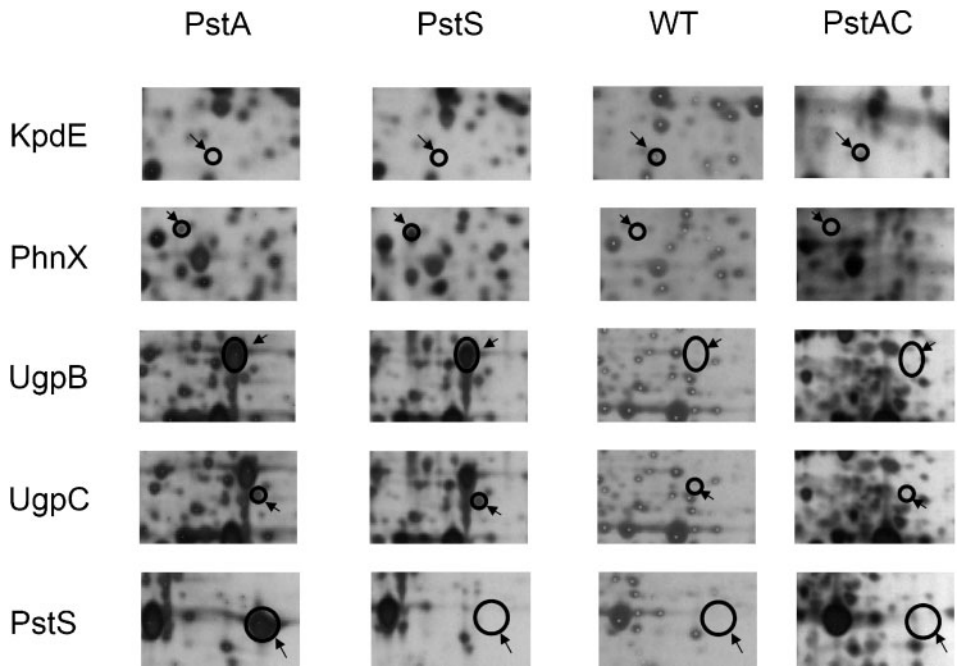

Fig. 6. Unique protein expression of the wild-type HI4320 strain and the *pst* mutant strains during planktonic growth in LB, as visualized by 2D PAGE. pH range 3–10 was utilized and the gels were silver-stained. Proteins were designated as being exclusively expressed if the spot was present in at least three separate gels. The transcription regulator KpdE was only expressed in the HI4320 wild-type strain. The phosphonoacetaldehyde phosphonohydrolase PhnX, periplasmic glycerol 3-phosphate binding protein UgpB, and *sn*-glycerol 3-phosphate transport ATP-binding protein UgpC were expressed in both *pst* mutants. The PstS protein was expressed exclusively by the *pstA* mutant. WT, *P. mirabilis* HI4320 strain; PstA, *P. mirabilis* HI4320 *pstA* strain; PstS, *P. mirabilis* HI4320 *pstS* strain; PstAC, *P. mirabilis* HI4320 *pstA* strain with pSMJ003 (pKHKS403 possessing the entire *pst* operon).

evaluated under planktonic and biofilm growth conditions and visualized by 2D PAGE. Several of the proteins exclusively expressed by these mutants were associated with phosphate assimilation and transport. However, our analyses have revealed proteins that may be involved in biofilm formation by *P. mirabilis* and thus also have a role in the attenuation of virulence of the *pst* mutant strains.

DISCUSSION

Mutagenesis studies have elucidated several potential roles for the Pst transport system in pathogenesis, the most intensively studied being the changes in cell surface properties that occur under low-phosphate conditions. Such changes include alterations in the polysaccharide content of the membrane (Mendrygal & Gonzalez, 2000; Ruberg *et al.*, 1999) and synthesis of phosphate-free membrane lipids [sulfolipids, ornithine-containing lipids, diacylglyceryl-*N*,*N*,*N*-trimethylhomoserine (DGTS) and teichoic acid], thought to conserve P_i during new membrane synthesis (Benning *et al.*, 1995; Danhorn *et al.*, 2004; Minnikin *et al.*, 1974; Soldo *et al.*, 1999). Other studies have postulated that the Pst system is involved in intracellular invasion: Tn*5* insertion mutants of the Δ*pstS* gene demonstrate a reduction in *hilA* and/or invasin gene expression in *Salmonella enterica* serotype Typhimurium (Lucas *et al.*, 2000). A Δ*pstS* insertional mutant in *Shigella flexneri* (Runyen-Janecky *et al.*, 2005) forms smaller plaques on Henle cell monolayers as compared with the wild-type; this correlates with the ability of the organism to cause disease, suggesting that the Pst system plays a role as an internal sensor of phosphate during cellular internalization. In *E. coli*, insertional mutants of the *pst* operon result in hyperinvasiveness to HEp-2 cells (Sinai & Bavoil, 1993). Some studies have suggested that *P. mirabilis* invades epithelial cells (Chippendale *et al.*, 1994; Oelschlaeger & Tall, 1996); thus, it may be that the Pst system has a role in invasion during UTIs.

Finally, there exists evidence – in other micro-organisms – that the Pst transport system plays a role in biofilm formation, critical for the establishment of chronic, catheter-associated UTIs. Studies using null mutants in *pstC* and *pstA* genes have revealed that the Pst system negatively regulates biofilm formation in *Pseudomonas aureofaciens* PA147-2 (Monds *et al.*, 2001). Since biofilm formation is critical for the establishment of *P. mirabilis* in the human host, mutations in the Pst system may explain

Table 5. Proteins expressed exclusively by the wild-type HI4320 or *pst* mutant strains during planktonic growth in LB

PMI number*	Protein	Function	Cellular location
Proteins expressed only in the wild-type strain			
1476	OppA1	ABC transporter	Periplasm
2021	GcvT	Glycine, serine, threonine metabolism	Cytoplasm
3299	IlvG	Valine, leucine, isoleucine biosynthesis	Cytoplasmic membrane
3551	PepQ	Degradation	Cytoplasm
601	YbhE	Hypothetical protein, 3-carboxymuconate cyclase	Unknown
2673	GntK	Putative glucokinase	Cytoplasm
420	LipA	Lipoic acid synthetase	Cytoplasm
1810	FadL	Long-chain fatty acid transporter	Outer membrane
2386	TerB	Tellurite resistance	Cytoplasm
3424	DeaD	Cold-shock RNA helicase	Cytoplasm
3455	PyrB	Aspartate carbamoyltransferase	Miscellaneous
2240	TruD	tRNA pseudouridine synthase D	Cytoplasm
2351	YgiC	Hypothetical protein, glutathionylspermidine synthase	Cytoplasm
3270	RplF	50S ribosomal subunit protein L6	Cytoplasm
3420	TruB	tRNA pseudouridine synthase B	Cytoplasm
868	YcfH	Highly similar to DNase YcfH	Unknown
2631	–	Undefined product, lipoprotein, putative	Unknown
2759	IclR	Putative IclR family transcriptional regulator	Unknown
2798	–	Hypothetical protein	Unknown
3673	AlbA	Putative MerR-family regulator	Periplasm
1226	KdpE	Transcriptional regulator of *kdp* operon	Cytoplasm
2883	NtrB	Nitrogen regulation protein NR(II)	Cytoplasm
Proteins expressed only in *pst* mutants			
361	–	Unknown	Unknown
2282	Frr	Ribosomal recycling factor	Cytoplasm
2893†	PstS	Phosphate-binding periplasmic protein precursor	Periplasm
3079	PhnX	Phosphonoacetaldehyde phosphonohydrolase	Cytoplasm
3296	–	Hypothetical protein	Cytoplasm
3357†	Orn	OligoRNase	Cytoplasm
3614	UgpC	*sn*-Glycerol 3-phosphate transport ATP-binding protein	Miscellaneous
3617	UgpB	Periplasmic glycerol 3-phosphate binding protein	Periplasm
3618	UgpQ	Glycerophosphoryl diester esterase	Cytoplasm
3715	–	Hypothetical protein	Unknown

*PMI – *Proteus mirabilis* index; a *P. mirabilis* genome databank hosted at the Sanger Institute, Cambridge, UK; http://www.sanger.ac.uk/Projects/P_mirabilis/.
†Expressed only in the *pstA* mutant. Proteins with no designation are left blank.

the observed attenuation of the mutant strains. This was the hypothesis under examination in our study.

The data presented in Fig. 2 support our hypothesis: c.f.u. recovered from biofilms of the Δ*pstA* and Δ*pstS* mutant strains were significantly lower than in the wild-type. Furthermore, these data were reinforced by CLSM imaging and COMSTAT analysis (Fig. 3, Table 3). The Δ*pstS* mutant strain showed marked reductions in biomass, mean thickness and maximum thickness, while the Δ*pstA* mutant showed a less marked reduction in mean thickness and maximum thickness when compared with the wild-type (Table 3). Qualitative visual analysis of *P. mirabilis* biofilm by CLSM lent support to these data (Fig. 3). Therefore, not surprisingly, mutations in both the *pstA* and the *pstS* genes caused a reduction in biofilm growth by *P. mirabilis* HI4320.

A comparison of protein expression during *P. mirabilis* biofilm growth in pooled human urine under flow by MALDI-TOF/TOF was performed to provide some insight into the biofilm growth defect displayed by the Δ*pstA* and Δ*pstS* mutants. The data tentatively identified 18 proteins as being expressed exclusively under these conditions: 16 in the *pst* mutants and two in wild-type HI4320 (Table 4). Of the 16 proteins present exclusively in the *pst* mutants, three were known members of the *pho* regulon, including the alkaline phosphatase PhoA, the periplasmic phosphate binding protein PstS, and the glycerol 3-phosphate periplasmic binding protein UgpB. These would be

expected to be upregulated in the *pst* mutant strains both because of the function of the *pho* regulon in phosphate uptake and because of the polarity of the mutants affecting expression of the genes downstream of the transposon insertion site, including *phoU*, a negative regulator of the *pho* regulon.

Other proteins expressed exclusively in the *pst* mutants may or may not be linked to biofilm formation. However, the functions of the upregulated proteins may aid our understanding of the cellular processes affected by the Pst system. Of interest are two proteins that have been shown in previous studies to be indirectly associated with the downregulation of biofilm formation (NagB and AphA). The glucosamine-6-phosphate isomerase NagB is part of the *nag* operon, whose genes are involved in the metabolism of *N*-acetylglucosamine 6-phosphate (GlcNAc6P), an important precursor of peptidoglycan and LPS synthesis. In *E. coli*, increases in the intracellular level of this precursor lead to the upregulation of the *nag* operon (Barnhart *et al.*, 2006) and downregulation of curli and type 1 pili (Barnhart *et al.*, 2006; Sohanpal *et al.*, 2004), both known to be involved in biofilm formation (Kikuchi *et al.*, 2005; Pratt & Kolter, 1998). Curli have been shown to assist in uroepithelial cell attachment in *E. coli* (Kikuchi *et al.*, 2005). It may be that expression of NagB was induced in the *pst* mutants as a method of acquiring additional nutrients. Since the expression of NagB – encoded by the first gene in the *nag* operon – is upregulated in the Δ*pst* mutants, type 1 pili may be downregulated, as occurs in *E. coli*. A homologue of the major type 1 pilin subunit FimA (PMI3435) is present in *P. mirabilis* HI4320. It is likely that downregulation of type 1 pili would negatively affect the ability of *pst* mutants to form biofilms.

The quorum-sensing-regulated activator AphA was also present in the proteomes of the Δ*pst* mutant biofilms cultured under flow in pooled human urine. This protein is known to regulate virulence determinants in *Vibrio cholerae* (Kovacikova *et al.*, 2005), in which it acts to prevent intracellular acidification during growth in glucose and at low pH as the organism is approaching stationary phase (Kovacikova *et al.*, 2005). Previous studies in *V. cholerae* have determined that AphA is indirectly involved in biofilm formation, as this protein reduces the intracellular c-di-GMP concentration, which in turn decreases biofilm formation (Kovacikova *et al.*, 2005). The acetoin reductase BudC, also expressed exclusively by the *pst* mutants, is involved in the 2,3-butanediol pathway, which protects the cell from acidification. These findings suggest that factors which may be important in biofilm formation are downregulated in the Δ*pst* mutants, thus providing an explanation for the observed defect in biofilm formation.

Four proteins exclusively expressed in the *pst* mutants were related to nutrient scavenging. The mutants expressed the aminopeptidases PepE and PepP. The aminobenzoyl-glutamate utilization protein AbgA is part of the *abg* operon involved in the catabolism of folate, a compound essential for the synthesis of DNA, RNA and amino acids (Carter *et al.*, 2007). The deoxyribose-phosphate aldolase DeoC is known to be important for the catabolism of deoxyribonucleosides (Han *et al.*, 2004). Lastly, the protein ArnB is known to be involved in LPS biosynthesis by modifying lipid A through the addition of 4-deoxy-L-arabinose (L-Ara4N) on phosphate residues (Breazeale *et al.*, 2005). Due to these modifications, *Proteus* spp. are not susceptible to cationic antimicrobial peptides. It is possible that although ArnB is being expressed, the addition of L-Ara4N is not possible due to the absence of phosphate residues on lipid A. If such modifications in LPS do indeed occur in *P. mirabilis* during times of phosphate limitation, they may affect the ability of these mutants to evade the immune response. Thus, these modifications in LPS structure may be partly or wholly responsible for the attenuation observed *in vivo*.

It has been suggested that the Δ*pst* mutants are defective in biofilm formation due to the constitutive induction of the genes of the *pho* regulon by PhoB. Currently, it is not known whether this defect is the direct result of the loss of the Pst system or is the indirect effect of the constitutive expression of the *pho* regulon. Numerous *pho* regulon genes have been identified (Torriani-Gorini, 1994). One gene that has been demonstrated to be involved in biofilm formation and is found to be upregulated during exponential phase in *pst* mutants is the general stress stationary-phase regulator RpoS (Ruiz & Silhavy, 2003).

RpoS regulates a number of genes involved in protecting the bacterial cell against various stresses (starvation, osmotic shock, pH, oxidative) (Hengge-Aronis, 2002). There have been conflicting reports about the function of RpoS during biofilm formation. Some have reported that RpoS expression is enhanced during biofilm formation (Adams & McLean, 1999; Xu *et al.*, 2001), while others have shown that mutations in the *rpoS* gene enhance biofilm formation (Corona-Izquierdo & Membrillo-Hernandez, 2002; Heydorn *et al.*, 2002; Yun *et al.*, 2007). It seems possible that RpoS is expressed transiently during some phase of biofilm development, as due to limited access to nutrients, bacterial growth rates within the centre of the biofilm – and especially deep inside microcolonies – are lower than those of bacteria located in the microcolony periphery (Moller *et al.*, 1996). A homologue of *rpoS* is present in the HI4320 genome (PMI2236) (data not shown). Thus, it seems possible that mutations in *pst* affect biofilm development through an *rpoS*-dependent mechanism, the precise nature of which is as yet unknown.

Thus, our data suggest that the *pst* operon has a role in the formation of biofilm by *P. mirabilis* and furthermore that this effect may be at least in part responsible for the attenuated virulence of the *pst* mutant strains. Proteomic analysis suggests that this is due to altered expression of one or more of a number of proteins differentially expressed in the mutant strains. Future studies will focus upon elucidating precisely which of these is involved in

biofilm formation and in the attenuated virulence of *P. mirabilis*.

ACKNOWLEDGEMENTS

We thank Anthony Haag at the Mass Spectrometry Core of the Biomolecular Resource Facility at the University of Texas Medical Branch for conducting MALDI-TOF MS and database analyses. This research was funded by the National Institute of Allergy and Infectious Diseases, National Institutes of Health grant R01-AI69568.

REFERENCES

Adams, J. L. & McLean, R. J. (1999). Impact of *rpoS* deletion on *Escherichia coli* biofilms. *Appl Environ Microbiol* **65**, 4285–4287.

Barnhart, M. M., Lynem, J. & Chapman, M. R. (2006). GlcNAc-6P levels modulate the expression of Curli fibers by *Escherichia coli*. *J Bacteriol* **188**, 5212–5219.

Belas, R. (1996). *Proteus mirabilis* swarmer cell differentiation and urinary tract infection. In *Urinary Tract Infections: Molecular Pathogenesis and Clinical Management*, pp. 271–298. Edited by H. L. Mobley & J. W. Warren. Washington, DC: American Society for Microbiology.

Benning, C., Huang, Z. H. & Gage, D. A. (1995). Accumulation of a novel glycolipid and a betaine lipid in cells of *Rhodobacter sphaeroides* grown under phosphate limitation. *Arch Biochem Biophys* **317**, 103–111.

Bradford, M. M. (1976). A rapid and sensitive method for the quantitation of microgram quantities of protein utilizing the principle of protein–dye binding. *Anal Biochem* **72**, 248–254.

Brady, R. A., Leid, J. G., Camper, A. K., Costerton, J. W. & Shirtliff, M. E. (2006). Identification of *Staphylococcus aureus* proteins recognized by the antibody-mediated immune response to a biofilm infection. *Infect Immun* **74**, 3415–3426.

Breazeale, S. D., Ribeiro, A. A., McClerren, A. L. & Raetz, C. R. (2005). A formyltransferase required for polymyxin resistance in *Escherichia coli* and the modification of lipid A with 4-amino-4-deoxy-L-arabinose. Identification and function of UDP-4-deoxy-4-formamido-L-arabinose. *J Biol Chem* **280**, 14154–14167.

Buckles, E. L., Wang, X., Lockatell, C. V., Johnson, D. E. & Donnenberg, M. S. (2006). PhoU enhances the ability of extraintestinal pathogenic *Escherichia coli* strain CFT073 to colonize the murine urinary tract. *Microbiology* **152**, 153–160.

Burall, L. S., Harro, J. M., Li, X., Lockatell, C. V., Himpsl, S. D., Hebel, J. R., Johnson, D. E. & Mobley, H. L. (2004). *Proteus mirabilis* genes that contribute to pathogenesis of urinary tract infection: identification of 25 signature-tagged mutants attenuated at least 100-fold. *Infect Immun* **72**, 2922–2938.

Carter, E. L., Jager, L., Gardner, L., Hall, C. C., Willis, S. & Green, J. M. (2007). *Escherichia coli abg* genes enable uptake and cleavage of the folate catabolite *p*-aminobenzoyl-glutamate. *J Bacteriol* **189**, 3329–3334.

Castelli, P., Caronno, R., Ferrarese, S., Mantovani, V., Piffaretti, G., Tozzi, M., Lomazzi, C., Rivolta, N. & Sala, A. (2006). New trends in prosthesis infection in cardiovascular surgery. *Surg Infect* (*Larchmt*) **7** (*suppl. 2*), S45–S47.

Chippendale, G. R., Warren, J. W., Trifillis, A. L. & Mobley, H. L. (1994). Internalization of *Proteus mirabilis* by human renal epithelial cells. *Infect Immun* **62**, 3115–3121.

Clauser, K. R., Baker, P. & Burlingame, A. L. (1999). Role of accurate mass measurement ($\pm$ 10 ppm) in protein identification strategies employing MS or MS/MS and database searching. *Anal Chem* **71**, 2871–2882.

Corona-Izquierdo, F. P. & Membrillo-Hernandez, J. (2002). A mutation in *rpoS* enhances biofilm formation in *Escherichia coli* during exponential phase of growth. *FEMS Microbiol Lett* **211**, 105–110.

Daigle, F., Fairbrother, J. M. & Harel, J. (1995). Identification of a mutation in the *pst-phoU* operon that reduces pathogenicity of an *Escherichia coli* strain causing septicemia in pigs. *Infect Immun* **63**, 4924–4927.

Danhorn, T., Hentzer, M., Givskov, M., Parsek, M. R. & Fuqua, C. (2004). Phosphorus limitation enhances biofilm formation of the plant pathogen *Agrobacterium tumefaciens* through the PhoR–PhoB regulatory system. *J Bacteriol* **186**, 4492–4501.

Delcher, A. L., Harmon, D., Kasif, S., White, O. & Salzberg, S. L. (1999). Improved microbial gene identification with GLIMMER. *Nucleic Acids Res* **27**, 4636–4641.

Gardy, J. L., Spencer, C., Wang, K., Ester, M., Tusnády, G. E., Simon, I., Hua, S., deFays, K., Lambert, C. & other authors (2003). PSORT-B: improving protein subcellular localization prediction for Gram-negative bacteria. *Nucleic Acids Res* **31**, 3613–3617.

Gharahdaghi, F., Weinberg, C. R., Meagher, D. A., Imai, B. S. & Mische, S. M. (1999). Mass spectrometric identification of proteins from silver-stained polyacrylamide gel: a method for the removal of silver ions to enhance sensitivity. *Electrophoresis* **20**, 601–605.

Gorg, A., Obermaier, C., Boguth, G., Harder, A., Scheibe, B., Wildgruber, R. & Weiss, W. (2000). The current state of two-dimensional electrophoresis with immobilized pH gradients. *Electrophoresis* **21**, 1037–1053.

Han, T. K., Zhu, Z. & Dao, M. L. (2004). Identification, molecular cloning, and sequence analysis of a deoxyribose aldolase in *Streptococcus mutans* GS-5. *Curr Microbiol* **48**, 230–236.

Hengge-Aronis, R. (2002). Signal transduction and regulatory mechanisms involved in control of the σ^S (RpoS) subunit of RNA polymerase. *Microbiol Mol Biol Rev* **66**, 373–395.

Heydorn, A., Nielsen, A. T., Hentzer, M., Sternberg, C., Givskov, M., Ersboll, B. K. & Molin, S. (2000). Quantification of biofilm structures by the novel computer program COMSTAT. *Microbiology* **146**, 2395–2407.

Heydorn, A., Ersboll, B., Kato, J., Hentzer, M., Parsek, M. R., Tolker-Nielsen, T., Givskov, M. & Molin, S. (2002). Statistical analysis of *Pseudomonas aeruginosa* biofilm development: impact of mutations in genes involved in twitching motility, cell-to-cell signaling, and stationary-phase sigma factor expression. *Appl Environ Microbiol* **68**, 2008–2017.

Jacobsen, S. M., Lane, M. C., Harro, J. M., Shirtliff, M. E. & Mobley, H. L. (2008). The high-affinity phosphate transporter Pst is a virulence factor for *Proteus mirabilis* during complicated urinary tract infection. *FEMS Immunol Med Microbiol* **52**, 180–193.

Jones, G. L., Muller, C. T., O'Reilly, M. & Stickler, D. J. (2006). Effect of triclosan on the development of bacterial biofilms by urinary tract pathogens on urinary catheters. *J Antimicrob Chemother* **57**, 266–272.

Kikuchi, T., Mizunoe, Y., Takade, A., Naito, S. & Yoshida, S. (2005). Curli fibers are required for development of biofilm architecture in *Escherichia coli* K-12 and enhance bacterial adherence to human uroepithelial cells. *Microbiol Immunol* **49**, 875–884.

Kovacikova, G., Lin, W. & Skorupski, K. (2005). Dual regulation of genes involved in acetoin biosynthesis and motility/biofilm formation by the virulence activator AphA and the acetate-responsive LysR-type regulator AlsR in *Vibrio cholerae*. *Mol Microbiol* **57**, 420–433.

Lamarche, M. G., Dozois, C. M., Daigle, F., Caza, M., Curtiss, R., III, Dubreuil, J. D. & Harel, J. (2005). Inactivation of the *pst* system reduces the virulence of an avian pathogenic *Escherichia coli* O78 strain. *Infect Immun* **73**, 4138–4145.

Lewis, K. (2001). Riddle of biofilm resistance. *Antimicrob Agents Chemother* **45**, 999–1007.

Lucas, R. L., Lostroh, C. P., DiRusso, C. C., Spector, M. P., Wanner, B. L. & Lee, C. A. (2000). Multiple factors independently regulate *hilA* and invasion gene expression in *Salmonella enterica* serovar Typhimurium. *J Bacteriol* **182**, 1872–1882.

Mathew, J. A., Tan, Y. P., Srinivasa Rao, P. S., Lim, T. M. & Leung, K. Y. (2001). *Edwardsiella tarda* mutants defective in siderophore production, motility, serum resistance and catalase activity. *Microbiology* **147**, 449–457.

Mendrygal, K. E. & Gonzalez, J. E. (2000). Environmental regulation of exopolysaccharide production in *Sinorhizobium meliloti*. *J Bacteriol* **182**, 599–606.

Minnikin, D. E., Abdolrahimzadeh, H. & Baddiley, J. (1974). Replacement of acidic phosphates by acidic glycolipids in *Pseudomonas diminuta*. *Nature* **249**, 268–269.

Mobley, H. L. (1996). Virulence of *Proteus mirabilis*. In *Urinary Tract Infections: Molecular Pathogenesis and Clinical Management*, pp. 245–269. Edited by H. L. Mobley & J. W. Warren. Washington, DC: American Society for Microbiology.

Mobley, H. L. & Warren, J. W. (1987). Urease-positive bacteriuria and obstruction of long-term urinary catheters. *J Clin Microbiol* **25**, 2216–2217.

Mobley, H. L., Island, M. D. & Massad, G. (1994). Virulence determinants of uropathogenic *Escherichia coli* and *Proteus mirabilis*. *Kidney Int Suppl* **47**, S129–S136.

Moller, S., Pedersen, A. R., Poulsen, L. K., Arvin, E. & Molin, S. (1996). Activity and three-dimensional distribution of toluene-degrading *Pseudomonas putida* in a multispecies biofilm assessed by quantitative *in situ* hybridization and scanning confocal laser microscopy. *Appl Environ Microbiol* **62**, 4632–4640.

Monds, R. D., Silby, M. W. & Mahanty, H. K. (2001). Expression of the Pho regulon negatively regulates biofilm formation by *Pseudomonas aureofaciens* PA147–2. *Mol Microbiol* **42**, 415–426.

Monds, R. D., Newell, P. D., Gross, R. H. & O'Toole, G. A. (2007). Phosphate-dependent modulation of c-di-GMP levels regulates *Pseudomonas fluorescens* Pf0–1 biofilm formation by controlling secretion of the adhesin LapA. *Mol Microbiol* **63**, 656–679.

Morris, N. S., Stickler, D. J. & McLean, R. J. (1999). The development of bacterial biofilms on indwelling urethral catheters. *World J Urol* **17**, 345–350.

Musher, D. M., Griffith, D. P., Yawn, D. & Rossen, R. D. (1975). Role of urease in pyelonephritis resulting from urinary tract infection with *Proteus*. *J Infect Dis* **131**, 177–181.

Oelschlaeger, T. A. & Tall, B. D. (1996). Uptake pathways of clinical isolates of *Proteus mirabilis* into human epithelial cell lines. *Microb Pathog* **21**, 1–16.

O'Farrell, P. H. (1975). High resolution two-dimensional electrophoresis of proteins. *J Biol Chem* **250**, 4007–4021.

Orihuela, C. J., Mills, J., Robb, C. W., Wilson, C. J., Watson, D. A. & Niesel, D. W. (2001). *Streptococcus pneumoniae* PstS production is phosphate responsive and enhanced during growth in the murine peritoneal cavity. *Infect Immun* **69**, 7565–7571.

O'Toole, G. A. & Kolter, R. (1998). Initiation of biofilm formation in *Pseudomonas fluorescens* WCS365 proceeds via multiple, convergent signalling pathways: a genetic analysis. *Mol Microbiol* **28**, 449–461.

O'Toole, G. A., Pratt, L. A., Watnick, P. I., Newman, D. K., Weaver, V. B. & Kolter, R. (1999). Genetic approaches to study of biofilms. *Methods Enzymol* **310**, 91–109.

Peerbooms, P. G., Verweij, A. M. & MacLaren, D. M. (1984). Vero cell invasiveness of *Proteus mirabilis*. *Infect Immun* **43**, 1068–1071.

Peirs, P., Lefèvre, P., Boarbi, S., Wang, X. M., Denis, O., Braibant, M., Pethe, K., Locht, C., Huygen, K. & Content, J. (2005). *Mycobacterium tuberculosis* with disruption in genes encoding the phosphate binding proteins PstS1 and PstS2 is deficient in phosphate uptake and demonstrates reduced *in vivo* virulence. *Infect Immun* **73**, 1898–1902.

Pratt, L. A. & Kolter, R. (1998). Genetic analysis of *Escherichia coli* biofilm formation: roles of flagella, motility, chemotaxis and type I pili. *Mol Microbiol* **30**, 285–293.

Rao, N. N. & Torriani, A. (1990). Molecular aspects of phosphate transport in *Escherichia coli*. *Mol Microbiol* **4**, 1083–1090.

Rosenberg, H., Gerdes, R. G. & Chegwidden, K. (1977). Two systems for the uptake of phosphate in *Escherichia coli*. *J Bacteriol* **131**, 505–511.

Ruberg, S., Puhler, A. & Becker, A. (1999). Biosynthesis of the exopolysaccharide galactoglucan in *Sinorhizobium meliloti* is subject to a complex control by the phosphate-dependent regulator PhoB and the proteins ExpG and MucR. *Microbiology* **145**, 603–611.

Ruiz, N. & Silhavy, T. J. (2003). Constitutive activation of the *Escherichia coli* Pho regulon upregulates *rpoS* translation in an Hfq-dependent fashion. *J Bacteriol* **185**, 5984–5992.

Runyen-Janecky, L. J., Boyle, A. M., Kizzee, A., Liefer, L. & Payne, S. M. (2005). Role of the Pst system in plaque formation by the intracellular pathogen *Shigella flexneri*. *Infect Immun* **73**, 1404–1410.

Sauer, K. & Camper, A. K. (2001). Characterization of phenotypic changes in *Pseudomonas putida* in response to surface-associated growth. *J Bacteriol* **183**, 6579–6589.

Sinai, A. P. & Bavoil, P. M. (1993). Hyper-invasive mutants define a novel Pho-regulated invasion pathway in *Escherichia coli*. *Mol Microbiol* **10**, 1125–1137.

Sohanpal, B. K., El-Labany, S., Lahooti, M., Plumbridge, J. A. & Blomfield, I. C. (2004). Integrated regulatory responses of *fimB* to *N*-acetylneuraminic (sialic) acid and GlcNAc in *Escherichia coli* K-12. *Proc Natl Acad Sci U S A* **101**, 16322–16327.

Soldo, B., Lazarevic, V., Pagni, M. & Karamata, D. (1999). Teichuronic acid operon of *Bacillus subtilis* 168. *Mol Microbiol* **31**, 795–805.

Soualhine, H., Brochu, V., Menard, F., Papadopoulou, B., Weiss, K., Bergeron, M. G., Legare, D., Drummelsmith, J. & Ouellette, M. (2005). A proteomic analysis of penicillin resistance in *Streptococcus pneumoniae* reveals a novel role for PstS, a subunit of the phosphate ABC transporter. *Mol Microbiol* **58**, 1430–1440.

Stickler, D. J., King, J. B., Winters, C. & Morris, S. L. (1993). Blockage of urethral catheters by bacterial biofilms. *J Infect* **27**, 133–135.

Stoodley, P., Sauer, K., Davies, D. G. & Costerton, J. W. (2002). Biofilms as complex differentiated communities. *Annu Rev Microbiol* **56**, 187–209.

Torriani-Gorini, A. (1994). Introduction: the *pho* regulon of *Escherichia coli*. In *Phosphate in Microbiology: Cellular and Molecular Biology*, pp. 1–4. Edited by S. Silver, A. Torriani-Gorini & E. Yagil. Washington, DC: American Society for Microbiology.

Walker, K. E., Moghaddame-Jafari, S., Lockatell, C. V., Johnson, D. & Belas, R. (1999). ZapA, the IgA-degrading metalloprotease of *Proteus mirabilis*, is a virulence factor expressed specifically in swarmer cells. *Mol Microbiol* **32**, 825–836.

Warren, J. W., Tenney, J. H., Hoopes, J. M., Muncie, H. L. & Anthony, W. C. (1982). A prospective microbiologic study of bacteriuria in

patients with chronic indwelling urethral catheters. *J Infect Dis* **146**, 719–723.

Xu, K. D., Franklin, M. J., Park, C. H., McFeters, G. A. & Stewart, P. S. (2001). Gene expression and protein levels of the stationary phase sigma factor, RpoS, in continuously-fed *Pseudomonas aeruginosa* biofilms. *FEMS Microbiol Lett* **199**, 67–71.

Yun, J. I., Cho, K. M., Kim, J. K., Lee, S. O., Cho, K. & Lee, K. (2007). Mutation of *rpoS* enhances *Pseudomonas* sp. KL28 growth at higher concentrations of *m*-cresol and changes its surface-related phenotypes. *FEMS Microbiol Lett* **269**, 97–103.

Edited by: V. Sperandio